Limitations of the Dilution Approximation for Concentrated Block Copolymer/Solvent Mixtures

J. R. Naughton and M. W. Matsen*

Polymer Science Centre, University of Reading, Whiteknights, Reading RG6 6AF, United Kingdom

Received December 19, 2001; Revised Manuscript Received April 10, 2002

ABSTRACT: Experimental control of block copolymer segregation is ideally achieved by varying temperature, but in practice, the range of segregation is very restricted. A far greater range can be accessed by diluting the block copolymer melt with a solvent, assuming the mixture obeys the so-called dilution approximation. We examine the accuracy of this dilution approximation as a function of solvent quality, size, and selectivity, using self-consistent field theory (SCFT). Naturally, the solvent quality must be good or else the solvent is prone to macrophase separation. Furthermore, the solvent size and selectivity must be sufficiently small so that the solvent distributes evenly throughout the mixture. We conclude by deriving a simple formula to specify the necessary constraints on the solvent size and selectivity.

I. Introduction

The phase behavior of AB diblock copolymer melts is, to a good approximation, controlled by the composition of the molecule f and the product χN, where N is the degree of polymerization and χ is the usual Flory−Huggins interaction parameter. The mean-field phase diagram for AB diblock copolymers is shown in Figure 1. From an experimental point of view, the exploration of this parameter space is difficult. In particular, changing either f or N requires the synthesis of an entirely new molecule. Although χ can be varied by changing temperature, in general, the range is rather restricted. If the temperature becomes too high, the polymer tends to degrade, while if it becomes too low, the melt solidifies due to either a glass transition or crystallization.

The difficulty of traversing the f axis of the phase diagram has been alleviated by a clever *one-component approximation* introduced by Bates et al.[3] In this case, two distinct diblock copolymers are synthesized, with compositions f_1 and f_2. According to the approximation, a blend of the two copolymers with volume fraction ϕ of the first copolymer behaves equivalently to a neat diblock copolymer melt with $f = f_{\text{eff}}$, where

$$f_{\text{eff}} = \phi f_1 + (1 - \phi) f_2 \tag{1}$$

Thus, the composition f can be varied continuously between f_1 and f_2 by simply adjusting ϕ. The validity of this approximation has since been justified by self-consistent-field theory (SCFT).[4] Provided that both diblock copolymers are of equal volume (i.e., same N) and similar in composition (i.e., $|f_1 - f_2| \lesssim 0.05$), the phase boundaries of the blend accurately coincide with those of the neat melt. Furthermore, the coexistence regions in the blend are sufficiently narrow that they can be safely ignored.

A similar trick to transverse the χN axis of the phase diagram, known as the *dilution approximation*, was proposed long ago by Helfand and Tagami.[5] This method involves diluting the diblock copolymer with a solvent.

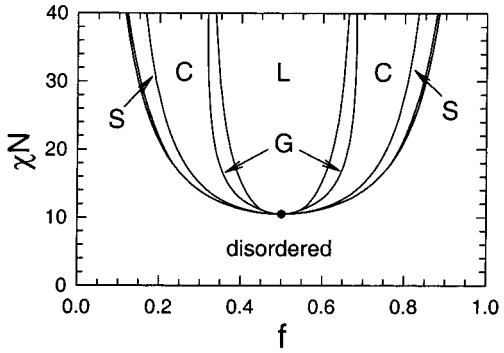

Figure 1. Theoretical phase diagram for neat AB diblock copolymer melts plotted as a function of segregation, χN, and composition, f.[1] The ordered phases are denoted lamellar (L), gyroid (G), cylindrical (C), and spherical (S). The solid dot denotes a mean-field critical point, which is ultimately destroyed by fluctuation effects.[2] In the dilution approximation, the diblock copolymer/solvent mixtures are mapped onto this diagram by setting $\chi = \chi_{\text{eff}} \equiv \phi\chi_{\text{AB}}$.

Of course, with the addition of a third chemical species, we now require three independent Flory−Huggins interaction parameters, χ_{AB}, χ_{AS}, and χ_{BS}, where A, B, and S denote A-type polymer, B-type polymer, and solvent, respectively. It is assumed that, for a relatively neutral solvent (i.e., $\chi_{\text{AS}} \approx \chi_{\text{BS}}$), a mixture with volume fraction ϕ of copolymer behaves equivalently to a neat diblock copolymer melt with $\chi = \chi_{\text{eff}}$, where

$$\chi_{\text{eff}} = \phi\chi_{\text{AB}} \tag{2}$$

This allows the segregation χN to be varied continuously over a much larger range than could be achieved by just changing temperature.

The dilution approximation has been used extensively in experiments.[6−13] Its validity relies on the assumption that the solvent distributes uniformly throughout the block copolymer structure. However, experiments[6] have indicated that even a slight degree of selectivity can lead to significant asymmetric swelling of the domains, thus

* To whom correspondence should be addressed.

10.1021/ma0122066 CCC: $22.00
Published on Web 06/04/2002

invalidating the dilution approximation. Even with a perfectly neutral solvent, there is a tendency for the solvent to accumulate at the interfaces. Huang et al.[7] have proposed a straightforward scattering experiment for qualifying the spatial uniformity of the solvent so as to assess the validity the dilution approximation. With appropriate solvents, the dilution approximation has been successful in predicting domain spacings,[8] scattering functions,[9] and order−order transitions (OOT's).[10,11] However, there is clear evidence that it fails for the order−disorder transition (ODT).[10−12]

Fredrickson and Leibler[14] performed the first theoretical test of the dilution approximation by examining AB diblock copolymers mixed with an athermal neutral solvent (i.e., $\chi_{AS} = \chi_{BS} = 0$). Because their calculation relied on weak-segregation approximations,[15] they focused on the ODT. Concentrated mixtures (i.e., $\phi \gtrsim 0.1$) were modeled using the standard fluctuation-corrected theory of Fredrickson and Helfand,[2] and semidilute mixtures (i.e., $\phi \lesssim 0.1$) were treated by supplementing this with the *blob* model.[16] Their results predicted that the position of the ODT would follow the dilution approximation in the concentrated regime but not in the semidilute regime. However, we now know that the ODT disobeys the dilution approximation in both regimes.[10−12] Fredrickson and Leibler also predicted that the two-phase coexistence regions would be completely negligible at weak segregations, and, in this case, experiments agree. Whitmore and co-workers[17,18] extended the test to stronger segregations by examining concentrated mixtures with good neutral solvent using self-consistent field theory (SCFT).[19] They found that the dilution approximation was valid for such cases, and that, in particular, the OOT's follow the expected dependence on ϕ, consistent with experiment.[10,11] We note that their OOT calculations[17] did not consider the possibility of coexistence regions.

These previous calculations focused on the ideal case where $\chi_{AS} = \chi_{BS}$. The question still remains, just how balanced must the solvent interactions be for the dilution approximation to remain valid. Although Banaszak and Whitmore[20] have demonstrated that some degree of selectivity can be tolerated, they did not specify how much. Previous studies also overlook the effect of solvent size. Here, we address both of these issues using SCFT, ultimately providing a simple criterion for estimating the limitations on solvent size and selectivity necessary for the validity of the dilution approximation.

II. Theory

In this section, we outline the self-consistent field theory (SCFT) for a mixture of n_c AB diblock copolymers with n_s solvent molecules. Each copolymer consists of N segments of which a fraction f forms the A block. We assume the mixture is incompressible with each polymer segment occupying a fixed volume ρ_0^{-1} and each solvent molecule taking a volume v_s. Thus, the total volume of the system is $V \equiv n_c N/\rho_0 + n_s v_s$, the volume fraction of copolymer is $\phi \equiv n_c N/V\rho_0$, and the ratio of the solvent to polymer size is $\alpha \equiv v_s\rho_0/N$. Furthermore, we assume that the A and B segments have the same statistical length a, although it is a trivial matter to extend our calculations to asymmetric lengths.[21]

SCFT begins by representing molecular interactions by effective fields.[22] For the present system, there are three fields

$$w_A(\mathbf{r}) = \chi_{AB}N\phi_B(\mathbf{r}) + \chi_{AS}N\phi_S(\mathbf{r}) + \xi(\mathbf{r}) \quad (3)$$

$$w_B(\mathbf{r}) = \chi_{AB}N\phi_A(\mathbf{r}) + \chi_{BS}N\phi_S(\mathbf{r}) + \xi(\mathbf{r}) \quad (4)$$

$$w_S(\mathbf{r}) = \chi_{AS}N\phi_A(\mathbf{r}) + \chi_{BS}N\phi_B(\mathbf{r}) + \xi(\mathbf{r}) \quad (5)$$

acting on the A segments, B segments, and solvent molecules, respectively. Here, $\phi_A(\mathbf{r})$, $\phi_B(\mathbf{r})$, and $\phi_S(\mathbf{r})$ are the standard dimensionless concentrations of these three respective components. Note that the field for each component has two contributions due to interactions with the other two components, and a Lagrange multiplier field $\xi(\mathbf{r})$ to enforce the incompressibility assumption,

$$\phi_A(\mathbf{r}) + \phi_B(\mathbf{r}) + \phi_S(\mathbf{r}) = 1 \quad (6)$$

The introduction of fields allows us to calculate the partition functions of the two different molecules. For the copolymer, we must first parametrize the molecule with a variable s that increases from 0 to 1 over its length.[22] This allows us to define a partial partition function, $q(\mathbf{r}, s)$, for the $(0, s)$ portion of the chain with the sth segment fixed at position $\boldsymbol{r}$. It is evaluated by solving the modified diffusion equation,

$$\frac{\partial}{\partial s}q(\mathbf{r}, s) = \begin{cases} \frac{1}{6}a^2N\nabla^2q(\mathbf{r}, s) - w_A(\mathbf{r})q(\mathbf{r}, s), & \text{if } s < f \\ \frac{1}{6}a^2N\nabla^2q(\mathbf{r}, s) - w_B(\mathbf{r})q(\mathbf{r}, s), & \text{if } f < s, \end{cases} \quad (7)$$

with the initial condition $q(\mathbf{r}, 0) = 1$.[19] A similar partial partition function, $q^\dagger(\mathbf{r}, s)$, is then calculated for the $(s, 1)$ portion of the chain. It satisfies eq 7 with the right-hand side multiplied by -1, and obeys the condition $q^\dagger(\mathbf{r}, 1) = 1$. In terms of these two functions, the total partition function for the copolymer molecule is

$$\mathcal{Q}_c = \int d\mathbf{r}\, q(\mathbf{r}, s)\, q^\dagger(\mathbf{r}, s) \quad (8)$$

Because the solvent molecule is treated as a point particle, its partition function is given by the simple expression

$$\mathcal{Q}_s = \int d\mathbf{r} \exp\{-\alpha w_S(\mathbf{r})\} \quad (9)$$

For a given set of fields, the dimensionless concentrations are

$$\phi_A(\mathbf{r}) = \frac{\phi V}{\mathcal{Q}_c}\int_0^f ds\, q(\mathbf{r}, s)\, q^\dagger(\mathbf{r}, s) \quad (10)$$

$$\phi_B(\mathbf{r}) = \frac{\phi V}{\mathcal{Q}_c}\int_f^1 ds\, q(\mathbf{r}, s)\, q^\dagger(\mathbf{r}, s) \quad (11)$$

$$\phi_S(\mathbf{r}) = \frac{(1-\phi)V}{\mathcal{Q}_s}\exp\{-\alpha w_S(\mathbf{r})\} \quad (12)$$

As in any mean-field calculation, the fields must be adjusted so that these concentrations satisfy the self-consistent eqs 3−6.

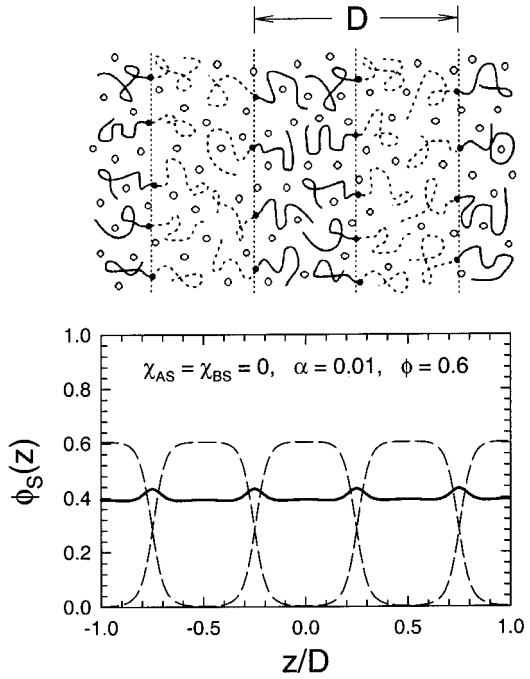

Figure 2. Schematic diagram showing the arrangement of solvent molecules (small open circles) within a diblock copolymer lamellar (L) phase of period D. Below is the solvent distribution calculated for $\chi_{AB}N = 50$, $f = 0.5$, $\chi_{AS} = \chi_{BS} = 0$, $\alpha = 0.01$, and $\phi = 0.6$. The A and B segment distributions of the diblock copolymer are indicated with dashed curves.

Once the fields have been self-consistently determined, the canonical free energy of the mixture is given by

$$\frac{NF}{k_B T \rho_0 V} = -\phi \ln\left(\frac{\mathcal{Q}_c}{V}\right) - \frac{1-\phi}{\alpha}\ln\left(\frac{\mathcal{Q}_s}{V}\right) - \frac{N}{V}\int d\mathbf{r}[\chi_{AB}\phi_A(\mathbf{r})\phi_B(\mathbf{r}) + \chi_{AS}\phi_A(\mathbf{r})\phi_S(\mathbf{r}) + \chi_{BS}\phi_B(\mathbf{r})\phi_S(\mathbf{r})] \quad (13)$$

For a periodic structure such as the lamellar phase, F has to be minimized with respect to the domain spacing, D (see Figure 2). Since our calculation is performed in the canonical ensemble, the free energy curvature must also be checked to ensure that $d^2F/d\phi^2 > 0$ for all ϕ. If the curvature is negative, the mixture will macrophase separate within an interval determined by a double-tangent construction.[23] Note that the grand-canonical ensemble[24] would be more convenient if macrophase separation was common, but in the present study it only occurs once.

III. Results

We begin by displaying in Figure 2 an actual solvent profile, $\phi_S(z)$, calculated by SCFT, where z denotes the coordinate normal to the lamellae and D equals the lamellar period. The dashed curves indicate the A and B segment profiles of the copolymer, $\phi_A(z)$ and $\phi_B(z)$, respectively. Naturally, the configurations of individual copolymer molecules are affected by both the level of segregation, $\phi_A(z) - \phi_B(z)$, and the solvent distribution, $\phi_S(z)$. The dilution approximation holds when the first contribution dominates the second. In mathematical terms, this requires $\sigma_{AB} \gg \sigma_S$, where we define the standard deviations,

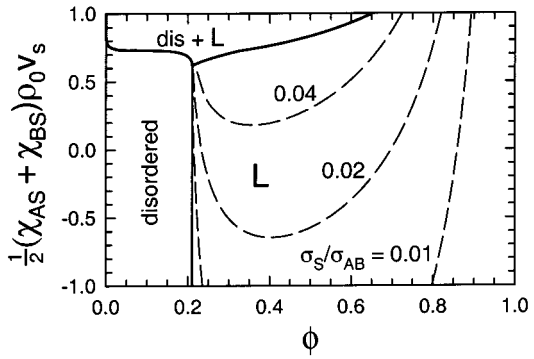

Figure 3. Phase diagram for a neutral solvent ($\chi_{AS} = \chi_{BS}$, $\alpha = 0.01$) mixed with a symmetric diblock copolymer ($\chi_{AB}N = 50$, $f = 0.5$) plotted in terms of copolymer volume fraction, ϕ, and solvent quality, $1/2(\chi_{AS} + \chi_{BS})\rho_0 v_s$. For good solvents, the lamellar (L) and disordered phases are separated by a continuous transition, whereas for poor solvents, they are separated by a two-phase coexistence region. The dashed curves in the L region represent contours of constant σ_S/σ_{AB}.

$$\sigma_S^2 \equiv \frac{1}{D}\int_0^D [\phi_S(z) - (1-\phi)]^2 \, dz \quad (14)$$

$$\sigma_{AB}^2 \equiv \frac{1}{D}\int_0^D [\phi_A(z) - \phi_B(z) - \phi(2f-1)]^2 dz \quad (15)$$

As we will demonstrate below, the dilution approximation is generally accurate when $\sigma_S/\sigma_{AB} \lesssim 0.01$, and remains moderately accurate up to $\sigma_S/\sigma_{AB} \approx 0.04$.

The vast parameter space (i.e., $\chi_{AB}N$, $\chi_{AS}N$, $\chi_{BS}N$, α, f, and ϕ) of diblock copolymer/solvent mixtures renders a complete survey of the system impractical. Therefore, we focus on a single representative diblock copolymer with $\chi_{AB}N = 50$ and $f = 0.5$. This segregation is chosen because it represents the approximate limit for which a copolymer sample can be disordered without entering the semidilute regime, where the underlying assumptions of SCFT are no longer valid. We have completed similar studies on a less segregated diblock copolymer ($\chi N = 25$) as well as asymmetric compositions ($f = 0.4$ and 0.3). However, these diblocks did not produce any notable differences and therefore will not be discussed in this particular section.

A. Solvent Quality. We begin by examining the effect of adding a neutral solvent (i.e., $\chi_{AS} = \chi_{BS}$) of relative size $\alpha = 0.01$ to the diblock copolymer sample. The phase diagram is plotted in Figure 3 as a function of copolymer volume fraction, ϕ, and solvent quality, $1/2(\chi_{AS} + \chi_{BS})\rho_0 v_s$. For a good solvent [i.e., $1/2(\chi_{AS} + \chi_{BS})\rho_0 v_s < 0.5$], the lamellar phase disorders at $\phi = 10.495/\chi_{AB}N = 0.21$ as expected from the dilution approximation. However, poor solvents tend to macrophase separate causing the order−disorder transition (ODT) to be replaced by a disordered + lamellar coexistence region.

To assess the extent over which the dilution approximation applies, contours of constant σ_S/σ_{AB} are plotted in the lamellar region of Figure 3. They indicate that the approximation is most accurate for good solvents, particularly near the ODT and at high copolymer concentrations. Figure 4 demonstrates that a reduction in solvent quality causes the solvent to accumulate at the A/B interfaces. Nevertheless, the spatial distribution of solvent remains reasonably uni-

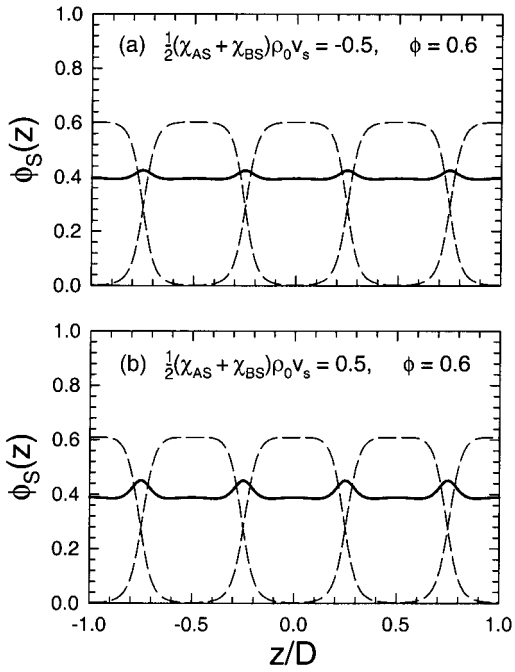

Figure 4. Distribution of a neutral solvent ($\chi_{AS} = \chi_{BS}$, $\alpha = 0.01$) within the lamellar phase of a symmetric diblock copolymer ($\chi_{AB}N = 50$, $f = 0.5$). The top (a) and bottom (b) plots are for good and Θ solvents, respectively. The polymer profiles are indicated with dashed curves.

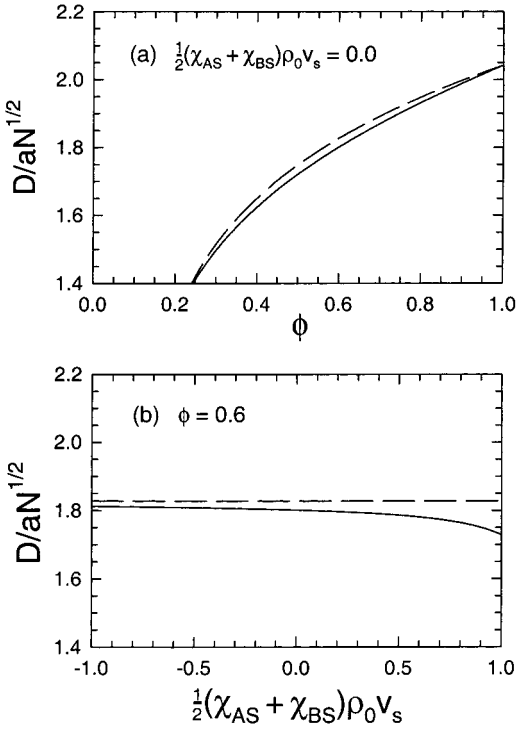

Figure 5. Comparison of the actual lamellar period (solid curves) to that predicted by the dilution approximation (dashed curves). Plots a and b correspond to horizontal and vertical paths across the phase diagram for mixtures of neutral solvent and symmetric diblock copolymer in Figure 3.

form even up to the point where macrophase separation occurs. This is consistent with previous studies,[17,18] suggesting that the dilution approximation is successful provided the solvent quality is good.

Figure 5 tests the accuracy of the dilution approximation by comparing the actual lamellar period (solid curves) to that predicted by the dilution approximation

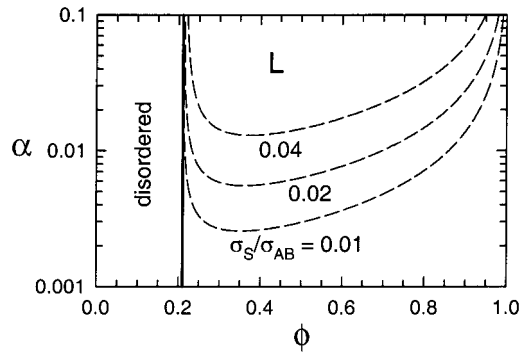

Figure 6. Phase diagram for an athermal neutral solvent ($\chi_{AS} = \chi_{BS} = 0$) mixed with symmetric diblock copolymer ($\chi_{AB}N = 50$, $f = 0.5$) plotted in terms of copolymer volume fraction, ϕ, and relative solvent size, $\alpha \equiv v_s\rho_0/N$. The solid line denotes a continuous transition between the lamellar (L) and disordered phases. The dashed curves in the L region represent contours of constant σ_S/σ_{AB}.

(dashed curves), i.e., the value obtained from a melt with $\chi = \phi\chi_{AB}$. As expected, the accuracy correlates well with σ_S/σ_{AB}. The predictions are accurate to within ~1% if $\sigma_S/\sigma_{AB} < 0.01$, and to within ~3% when $\sigma_S/\sigma_{AB} < 0.04$.

B. Solvent Size. Because of an unfortunate convention that we will discuss later, the effect of solvent size has been overlooked in the past. We now examine it for mixtures of neutral athermal solvent (i.e., $\chi_{AS} = \chi_{BS} = 0$). Figure 6 shows the resulting phase diagram plotted as a function of copolymer volume fraction, ϕ, and relative solvent size, $\alpha \equiv v_s\rho_0/N$. Again, the dilution approximation correctly predicts the ODT at $\phi = 0.21$. Because the quality of athermal solvents is classified as good, there are no instances of macrophase separation.

The contours of constant σ_S/σ_{AB} plotted in the L region of Figure 6 indicate that the dilution approximation worsens as the solvent molecules increase in size, even though the solvent quality remains constant. Indeed, Figure 7 demonstrates that the larger solvent molecules have a greater tendency to migrate to the interface.

As before, we test the dilution approximation by comparing actual and predicted domain spacings. Figure 8 clearly demonstrates that the approximation deteriorates as σ_S/σ_{AB} increases. The agreement is again within ~1% for $\sigma_S/\sigma_{AB} < 0.01$, and ~3% for $\sigma_S/\sigma_{AB} < 0.04$.

C. Solvent Selectivity. Last, we consider a selective solvent with $\chi_{AS} = -\chi_{BS}$ and $\alpha = 0.01$. Figure 9 shows the phase diagram plotted as a function of copolymer volume fraction, ϕ, and solvent selectivity, $(\chi_{AS} - \chi_{BS})\rho_0 v_s$. In this case, the ODT fails to obey the dilution approximation. Instead, the selectivity has a stabilizing effect on the ordered lamellar phase,[6,20] pushing the ODT toward low concentrations (i.e., $\phi < 0.21$).

The contours of constant σ_S/σ_{AB} plotted in the L region of Figure 9 demonstrate that a slight solvent selectivity is generally sufficient to invalidate the dilution approximation. As is clearly evident from Figure 10, this is because the selectivity has a dramatic effect on the relative swelling of the A and B domains. We note that in the region where σ_S/σ_{AB} is large, this asymmetric swelling could stabilize other ordered phases (i.e., G, C, and S from Figure 1).[10] However, our present interest lies only in the region where σ_S/σ_{AB} is small, and therefore, these alternative phases are not considered.

Figure 11 demonstrates that the asymmetric swelling causes a severe failure in the ability of the dilution

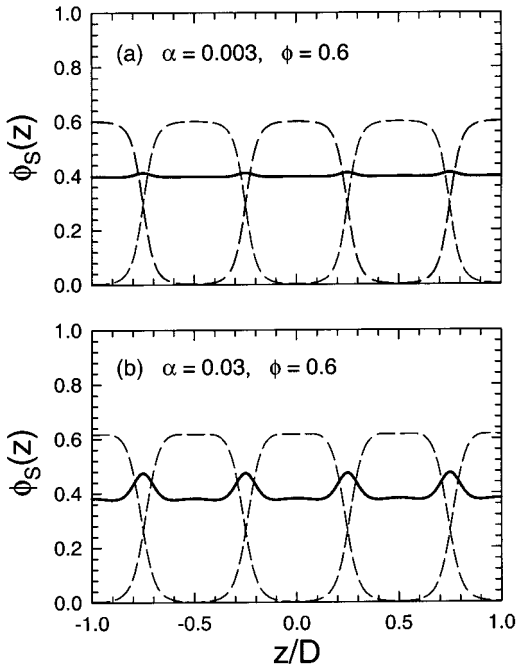

Figure 7. Distribution of an athermal neutral solvent ($\chi_{AS} = \chi_{BS} = 0$) within the lamellar phase of a symmetric diblock copolymer ($\chi_{AB}N = 50$, $f = 0.5$). The top (a) and bottom (b) plots correspond to small and large solvent molecules, respectively. The polymer profiles are indicated with dashed curves.

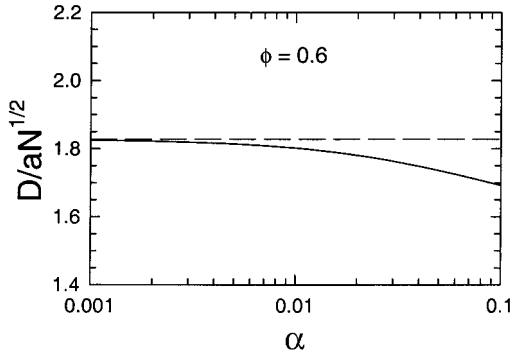

Figure 8. Comparison of the actual lamellar period (solid curves) to that predicted by the dilution approximation (dashed curves). This plot corresponds to a vertical path across the phase diagram in Figure 6 for mixtures of athermal neutral solvent and symmetric diblock copolymer.

approximation to predict the domain spacing. Nevertheless, the inaccuracy still correlates with σ_S/σ_{AB} as it did before; ~3% accuracy is again achieved if $\sigma_S/\sigma_{AB} < 0.04$, while ~1% accuracy requires $\sigma_S/\sigma_{AB} < 0.01$.

IV. Discussion

The reason that uniform solvent distributions give rise to the dilution approximation is evident from the mathematical form of eqs 3 and 4 for $w_A(\mathbf{r})$ and $w_B(\mathbf{r})$. Since additive constants have no effect on the statistical mechanics of the copolymer, the solvent contribution to $w_A(\mathbf{r})$ and $w_B(\mathbf{r})$ can be ignored in the limit of uniform $\phi_S(\mathbf{r})$. In that case, eqs 3 and 4 reduce to those of the neat melt,[22] except that, in the mixture, the polymer concentrations are reduced by a factor ϕ. However, since χ_{AB} only enters the theory through the field equations as a factor multiplying the polymer concentrations, the reduction in polymer concentration is exactly equivalent to a reduction in χ_{AB} by the same factor, ϕ. Hence, a

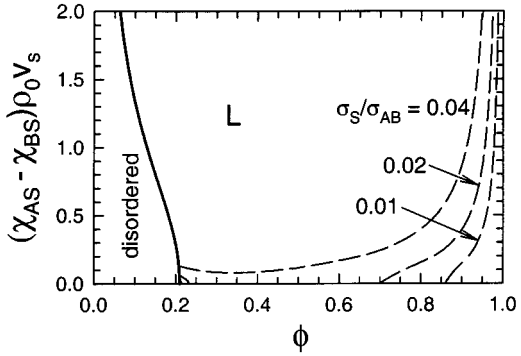

Figure 9. Phase diagram for a selective solvent ($\chi_{AS} = -\chi_{BS}$, $\alpha = 0.01$) mixed with symmetric diblock copolymer ($\chi_{AB}N = 50$ and $f = 0.5$) plotted in terms of copolymer volume fraction, ϕ, and solvent selectivity, $(\chi_{AS} - \chi_{BS})\rho_0 v_s$. The solid curve denotes a continuous transition between the lamellar (L) and disordered phases. The dashed curves in the L region represent contours of constant σ_S/σ_{AB}.

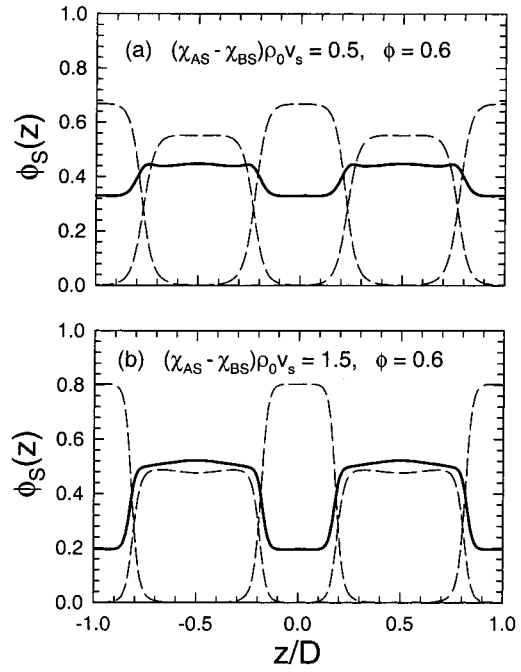

Figure 10. Distribution of a selective solvent ($\chi_{AS} = -\chi_{BS}$, $\alpha = 0.01$) mixed with symmetric diblock copolymer ($\chi_{AB}N = 50$, $f = 0.5$). The top (a) and bottom (b) plots correspond to weak and strong selectivities, respectively. The polymer profiles are indicated with dashed curves.

diluted mixture with $\phi_A(\mathbf{r}) + \phi_B(\mathbf{r}) = \phi$ is equivalent to a melt with $\chi = \chi_{eff} \equiv \phi\chi_{AB}$.

The necessary conditions for a uniform solvent distribution follow from eq 12, where it is immediately obvious that the spatial variations in $\phi_S(\mathbf{r})$ are directly linked to those in $\alpha w_S(\mathbf{r})$. Thus, the need for small α is clear. It is also not too difficult to see that $\chi_{AS} \approx \chi_{BS}$ is required, or else the terms $\chi_{AS}N\phi_A(\mathbf{r}) + \chi_{BS}N\phi_B(\mathbf{r})$, in the expression for $w_S(\mathbf{r})$, will exhibit significant oscillations. Notice that the solvent quality is relatively unimportant, provided that it is not so poor as to cause macrophase separation. The necessary constraints on solvent size and selectivity are easily determined from plots like that in Figure 12, where contours of constant σ_S/σ_{AB} are plotted as a function of α and $|\chi_{AS} - \chi_{BS}|\rho_0 v_s$. High accuracy requires the solvent parameters to fall within the $\sigma_S/\sigma_{AB} \approx 0.01$ contour, while moderate accuracy requires $\sigma_S/\sigma_{AB} \lesssim 0.04$.

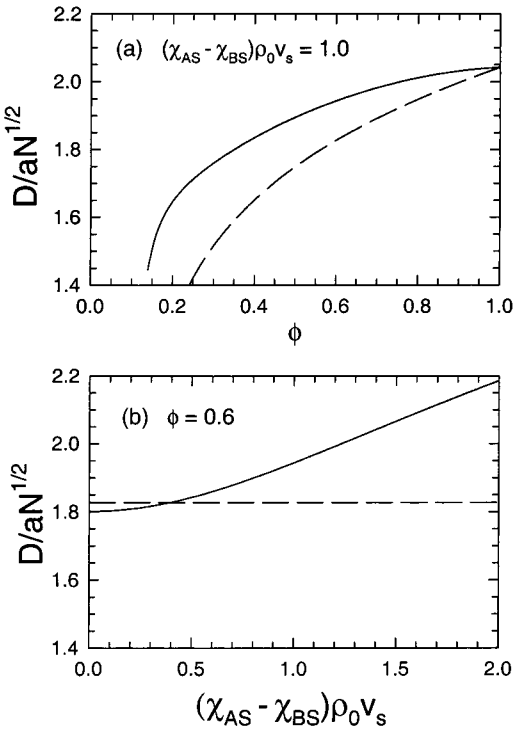

Figure 11. Comparison of the actual lamellar period (solid curves) to that predicted by the dilution approximation (dashed curves). Plots (a) and (b) correspond to horizontal and vertical paths across the phase diagram in Figure 9 for mixtures of selective solvent and symmetric diblock copolymer.

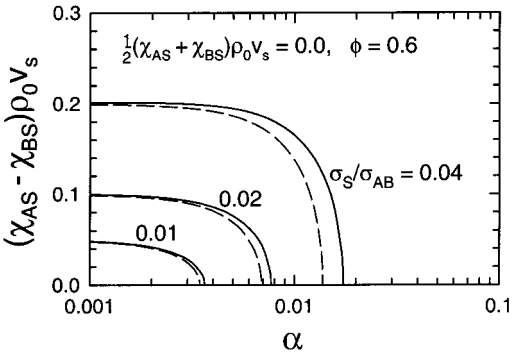

Figure 12. Contours of constant σ_S/σ_{AB} for mixtures of selective solvent ($\chi_{AS} = -\chi_{BS}$) and symmetric diblock copolymer ($\chi_{AB}N = 50$, $f = 0.5$). The solid curves correspond to full SCFT calculations, while the dashed curves are obtained from eq 21 using $\Sigma_\xi/\Sigma_{AB} = 4.355$.

The obvious problem with Figure 12 is that it only applies to very specific mixtures, i.e., $\chi_{AS} + \chi_{BS} = 0.0$, $\phi = 0.6$, $\chi_{AB}N = 50$, and $f = 0.5$. Fortunately, it is possible to derive a general expression for estimating small values of σ_S/σ_{AB}. When σ_S/σ_{AB} is small, we can safely assume $\phi_A(\mathbf{r}) + \phi_B(\mathbf{r}) \approx \phi$, in which case

$$w_S(\mathbf{r}) \approx \frac{1}{2}(\chi_{AS} - \chi_{BS})N(\phi_A(\mathbf{r}) - \phi_B(\mathbf{r})) + \xi(\mathbf{r}) + \text{constant} \quad (16)$$

where the value of the constant is unimportant. In the spirit of the dilution approximation, $\phi_A(\mathbf{r}) - \phi_B(\mathbf{r})$ and $\xi(\mathbf{r})$ can be estimated from neat diblock copolymer melts using $\chi = \chi_{eff} \equiv \phi\chi_{AB}$. However, we must account for the fact that the polymer concentrations are reduced by a factor ϕ, and thus eq 16 becomes

$$w_S(\mathbf{r}) \approx \frac{1}{2}\phi(\chi_{AS} - \chi_{BS})N[\phi_A(\mathbf{r}) - \phi_B(\mathbf{r}) - (2f - 1)] + [\xi(\mathbf{r}) - \xi_0] \quad (17)$$

where ξ_0 is the average value of $\xi(\mathbf{r})$. For convenience, the arbitrary constant in eq 16 has been set so that the average of $w_S(\mathbf{r})$ is zero. We also know from eq 12 that

$$\phi_S(\mathbf{r}) \propto \exp\{-\alpha w_S(\mathbf{r})\} \approx 1 - \alpha w_S(\mathbf{r}) \quad (18)$$

where the Taylor series approximation is valid for $\sigma_S/\sigma_{AB} \ll 1$. Since the average of $w_S(\mathbf{r})$ has been adjusted to zero, the normalized concentration is just

$$\phi_S(\mathbf{r}) \approx (1 - \phi)(1 - \alpha w_S(\mathbf{r})) \quad (19)$$

Inserting eqs 17 and 19 into eq 14 yields

$$\sigma_S^2 = \left(\frac{1}{2}(1 - \phi)\phi(\chi_{AS} - \chi_{BS})\rho_0 v_s \Sigma_{AB}\right)^2 + ((1 - \phi)\Sigma_\xi \alpha)^2 \quad (20)$$

where Σ_ξ and Σ_{AB} are the standard deviations of $\xi(\mathbf{r})$ and $\phi_A(\mathbf{r}) - \phi_B(\mathbf{r})$, respectively, evaluated for a neat diblock copolymer melt with $\chi = \chi_{eff} \equiv \phi\chi_{AB}$. Note that the average of $[\phi_A(\mathbf{r}) - \phi_B(\mathbf{r}) - (2f - 1)][\xi(\mathbf{r}) - \xi_0]$ has been ignored. It is identically zero when $f = 0.5$ and remains negligible even when $f \neq 0.5$. On the basis of the dilution approximation, it also follows that $\sigma_{AB} \approx \phi\Sigma_{AB}$, and thus

$$\left(\frac{\sigma_S}{\sigma_{AB}}\right)^2 = \left(\frac{1 - \phi}{2}(\chi_{AS} - \chi_{BS})\rho_0 v_s\right)^2 + \left(\frac{1 - \phi}{\phi}\frac{\Sigma_\xi}{\Sigma_{AB}}\alpha\right)^2 \quad (21)$$

The dashed curves in Figure 12 demonstrate that indeed eq 21 provides an adequate estimate of σ_S/σ_{AB}. Thus, we can now assess the validity of the dilution approximation without performing a SCFT calculation. All we require is the ratio Σ_ξ/Σ_{AB}, which is provided in Figure 13. We note that the derivation of eq 21 does not assume any particular morphology and thus applies equally well to nonlamellar phases.

Not only does eq 21 summarize what would otherwise require a tremendous number of numerical calculations, but it also allows us to easily understand how the six parameters of the diblock copolymer/solvent mixtures influence the validity of the dilution approximation. Interestingly, the parameters specific to the diblock copolymer (i.e., $\chi_{AB}N$ and f) only enter indirectly through their influence on Σ_ξ/Σ_{AB}. On the basis of Figure 13, this ratio depends strongly on the segregation of the corresponding neat diblock copolymer melt but hardly at all on either its composition f or its morphology. In fact, we should have expected this. Any tendency for solvent molecules to preferentially accumulate in either the A-rich, B-rich, or interfacial region should depend primarily on the energetics and not on the size or shape of the domains.

Since the dilution approximation is based on the form of the self-consistent field equations, we cannot expect it to apply if the underlying assumptions of SCFT are not met. For example, SCFT treats the individual polymer segments as ideal springs, which assumes that their internal configurations obey random-walks statistics.[22] However, at semidilute concentrations (i.e., $\phi \sim 0.1$), the polymer chains begin to obey self-avoiding statistics up to lengths comparable to the distance

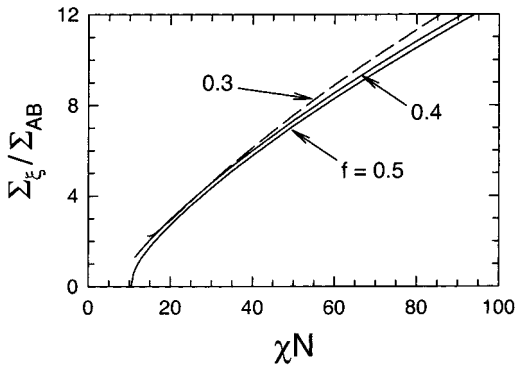

Figure 13. Ratio of the standard deviations for $\xi(\mathbf{r})$ and $\phi_A(\mathbf{r}) - \phi_B(\mathbf{r})$ calculated for a neat diblock copolymer melt as a function of segregation, χN, at three different compositions, f. The solid and dashed curves are calculated for lamellar and cylindrical morphologies, respectively. The values to be inserted into eq 21 are obtained by setting $\chi = \chi_{eff} \equiv \phi\chi_{AB}$.

between interchain contacts.[16] Indeed, calculations by Fredrickson and Leibler[14] and by Olvera de la Cruz[26] using the blob model predict that the simple dilution approximation does not apply at semidilute concentrations. Experiments[27] agree with this conclusion, although they also suggest that the predictions from the blob model are qualitatively inaccurate.

The validity of SCFT also assumes that the polymer and solvent molecules are randomly mixed on the local scale, or, in other words, that the short-range polymer−solvent correlations are weak. This is because SCFT assumes, for example, $\langle\hat{\phi}_A(\mathbf{r})\hat{\phi}_S(\mathbf{r})\rangle \approx \phi_A(\mathbf{r})\phi_S(\mathbf{r})$, where $\hat{\phi}_A(\mathbf{r})$ and $\hat{\phi}_S(\mathbf{r})$ are instantaneous concentrations and $\phi_A(\mathbf{r}) \equiv \langle\hat{\phi}_A(\mathbf{r})\rangle$ and $\phi_S(\mathbf{r}) \equiv \langle\hat{\phi}_S(\mathbf{r})\rangle$ are the ensemble-averaged concentrations. To avoid strong correlations, the energy difference, $\Delta E = k_B T\chi_{AS}\rho_0 v_s$, between placing a single solvent molecule in an A-rich region and a solvent-rich region should not exceed the thermal energy, $k_B T$. Thus, we require $\chi_{AS}\rho_0 v_s \gtrsim -1$, and similarly $\chi_{BS}\rho_0 v_s \gtrsim -1$.

It is well-known that SCFT is inaccurate near the mean-field critical point in Figure 1, because it ignores important Brazovskii fluctuations.[22] Nevertheless, the fluctuation-corrected calculation by Fredrickson and Leibler[14] suggests that the dilution approximation remains valid along the ODT for concentrated mixtures. However, experiments[10−12] have strongly disputed this claim. This, in fact, supports emerging evidence[28] that the current method[2] of correcting for fluctuations is unreliable.[22]

In this paper, we have deviated from the standard convention for polymer solutions of setting the reference volume, ρ_0^{-1}, equal to the volume of a solvent molecule, v_s. Although this practice is completely legitimate, it is also a recipe for confusion,[25] since the value chosen for ρ_0 affects the Flory−Huggins interaction parameters, the polymerization indices, and the statistical segment lengths (i.e., χ, N, and a). Instinctively, we might expect that if the same diblock copolymer was mixed with two different solvents (e.g., diblock + toluene and diblock + cyclohexane), then the block copolymer parameters, χ_{AB}, N, and a, would remain the same for both mixtures. However, this is not the case when the reference volume has to change to match the solvent size. Furthermore, the practice of setting $\rho_0^{-1} = v_s$ obscures the dependence of solvent size, v_s, on the phase behavior, which explains why its effect has been overlooked in the past. Now that continuum models have replaced lattice models, it seems best to abandon the convention of setting $\rho_0 v_s = 1$.

V. Conclusion

The present study has theoretically examined the validity of the dilution approximation as a tool for lowering the level of segregation, χN, in a block copolymer melt. According to this approximation, a mixture with copolymer volume fraction ϕ behaves equivalently to a neat diblock copolymer melt with $\chi = \chi_{eff} \equiv \phi\chi_{AB}$. The validity of this approximation hinges on the assumption that the solvent distribution, $\phi_S(\mathbf{r})$, is uniform relative to the polymer segregation, $\phi_A(\mathbf{r}) - \phi_B(\mathbf{r})$. More specifically, the dilution approximation is generally accurate provided $\sigma_S/\sigma_{AB} \lesssim 0.01$, where σ_S and σ_{AB} are the standard deviations of $\phi_S(\mathbf{r})$ and $\phi_A(\mathbf{r}) - \phi_B(\mathbf{r})$, respectively. In fact, the accuracy remains reasonable even up to $\sigma_S/\sigma_{AB} \approx 0.04$.

For a given copolymer sample, the effect of an added solvent depends on its average quality $(f\chi_{AS} + (1 - f)\chi_{BS})\rho_0 v_s$, its relative size $\alpha \equiv v_s\rho_0/N$, and its selectivity $(\chi_{AS} - \chi_{BS})\rho_0 v_s$. The validity of the dilution approximation first requires the solvent quality to be good [i.e., $(f\chi_{AS} + (1 - f)\chi_{BS})\rho_0 v_s < 0.5$], or else the solvent is prone to macrophase separation from the copolymer. Second, the above constraint on σ_S/σ_{AB} requires the solvent size and selectivity to be sufficiently small as determined by eq 21 using the ratio Σ_ξ/Σ_{AB} plotted in Figure 13. This latter ratio depends strongly on the effective segregation, $\chi_{eff}N$, but hardly at all on the diblock composition, f, or the symmetry of the morphology.

Even if the above criteria are met, we cannot expect the dilution approximation to apply when the assumptions of SCFT are not fulfilled. For example, the approximation is expected to fail when the copolymer concentration becomes semidilute (i.e., $\phi \lesssim 0.1$), since this causes the local polymer configurations to switch from random-walk to self-avoiding statistics. Furthermore, if the solvent is too good (i.e., $\chi_{AS}\rho_0 v_s \lesssim -1$ or $\chi_{BS}\rho_0 v_s \lesssim -1$), the strong polymer−solvent correlations will invalidate the local mixing assumption used to approximate the internal energy. Because SCFT ignores fluctuation effects, our conclusions cannot be extended to the ODT. Indeed, experiments[12] have demonstrated that the dilution approximation fails in this regime. Nevertheless, there remains a wide range of parameter space where the dilution approximation can be trusted, and thus it still constitutes a valuable tool for manipulating block copolymer segregation.

Acknowledgment. This work was supported by the EPSRC (GR/M22130) and by the Dow Chemical Co.

Appendix: Analytical Determination of the ODT

Fredrickson and Leibler[14] derived analytical expressions for the mean-field ODT using the random phase approximation. Here, we show that equivalent expressions emerge more simply by performing a first-order harmonic approximation of the SCFT equations. To

start, the fields, concentrations, and partial partition functions are approximated as

$$w_\alpha(z) \approx w_{\alpha,1}\sqrt{2}\cos(kz) \tag{22}$$

$$\phi_\alpha(z) \approx \phi_{\alpha,0} + \phi_{\alpha,1}\sqrt{2}\cos(kz) \tag{23}$$

$$q(z, s) \approx q_0(s) + q_1(s)\sqrt{2}\cos(kz) \tag{24}$$

$$q^\dagger(z, s) \approx q_0^\dagger(s) + q_1^\dagger(s)\sqrt{2}\cos(kz) \tag{25}$$

where $k \equiv 2\pi/D$ and α represents A, B, or S. Then from the modified diffusion eq 7, it follows that

$$\frac{\mathrm{d}}{\mathrm{d}s}q_0(s) = \begin{cases} -w_{\mathrm{A},1}q_1(s), & \text{if } 0 < s < f \\ -w_{\mathrm{B},1}q_1(s), & \text{if } f < s < 1 \end{cases} \tag{26}$$

$$\frac{\mathrm{d}}{\mathrm{d}s}q_1(s) = \begin{cases} -xq_1(s) - w_{\mathrm{A},1}q_0(s), & \text{if } 0 < s < f \\ -xq_1(s) - w_{\mathrm{B},1}q_0(s), & \text{if } f < s < 1 \end{cases} \tag{27}$$

where $x \equiv k^2a^2N/6$. Furthermore, the initial condition $q(z, 0) = 1$ implies that $q_0(0) = 1$ and $q_1(0) = 0$. At this point, we solve eq 27 for $q_1(s)$ using the approximation $q_0(s) \approx 1$, and then we solve eq 26 to improve the approximation for $q_0(s)$. This provides us with

$$q(z, f) \approx 1 + \frac{1}{2}{w_{\mathrm{A},1}}^2 g(f, x) - w_{\mathrm{A},1}h(f, x)\sqrt{2}\cos(kz) \tag{28}$$

where

$$g(f, x) = 2(\exp(-fx) - 1 + fx)/x^2 \tag{29}$$

$$h(f, x) = (1 - \exp(-fx))/x \tag{30}$$

Repeating this procedure for $q^\dagger(z, s)$ gives

$$q^\dagger(z, f) \approx 1 + \frac{1}{2}{w_{\mathrm{B},1}}^2 g(1 - f, x) - w_{\mathrm{B},1}h(1 - f, x)\sqrt{2}\cos(kz) \tag{31}$$

With these relationships, we evaluate the partition functions of the copolymer and solvent to quadratic order in the fields:

$$\frac{\mathcal{Q}_\mathrm{c}}{V} \approx 1 + \frac{1}{2}S_{11}{w_{\mathrm{A},1}}^2 + \frac{1}{2}S_{22}{w_{\mathrm{B},1}}^2 + S_{12}w_{\mathrm{A},1}w_{\mathrm{B},1} \tag{32}$$

$$\frac{\mathcal{Q}_\mathrm{s}}{V} \approx 1 + \frac{1}{2}{w_{\mathrm{S},1}}^2\alpha^2 \tag{33}$$

where $S_{11} = g(f, x)$, $S_{22} = g(1 - f, x)$, and $S_{12} = h(f, x)h(1 - f, x)$. The concentrations are then found by differentiating eqs 32 and 33 according to

$$\phi_{\mathrm{A},1} = -\phi\frac{\partial \ln \mathcal{Q}_\mathrm{c}}{\partial w_{\mathrm{A},1}} = -\phi[S_{11}w_{\mathrm{A},1} + S_{12}w_{\mathrm{B},1}] \tag{34}$$

$$\phi_{\mathrm{B},1} = -\phi\frac{\partial \ln \mathcal{Q}_\mathrm{c}}{\partial w_{\mathrm{B},1}} = -\phi[S_{22}w_{\mathrm{B},1} + S_{12}w_{\mathrm{A},1}] \tag{35}$$

$$\phi_{\mathrm{S},1} = -\frac{(1 - \phi)}{\alpha}\frac{\partial \ln \mathcal{Q}_\mathrm{s}}{\partial w_{\mathrm{S},1}} = -(1 - \phi)w_{\mathrm{S},1}\alpha \tag{36}$$

Inverting these equations for the fields gives

$$w_{\mathrm{A},1} = \frac{S_{12}\phi_{\mathrm{B},1} - S_{22}\phi_{\mathrm{A},1}}{\det(S)\phi} \tag{37}$$

$$w_{\mathrm{B},1} = \frac{S_{12}\phi_{\mathrm{A},1} - S_{11}\phi_{\mathrm{B},1}}{\det(S)\phi} \tag{38}$$

$$w_{\mathrm{S},1} = -\frac{\phi_{\mathrm{S},1}}{\alpha(1 - \phi)} \tag{39}$$

where $\det(S) = S_{11}S_{22} - S_{12}^2$. Now, it is just a matter of inserting the above expressions for $\mathcal{Q}_\mathrm{c}$, $\mathcal{Q}_\mathrm{s}$, $w_\mathrm{A}(\mathbf{r})$, $w_\mathrm{B}(\mathbf{r})$, and $w_\mathrm{S}(\mathbf{r})$ into the free energy equation, eq 13, expanding the logarithms, and replacing $\phi_{\mathrm{S},1}$ by $-(\phi_{\mathrm{A},1} + \phi_{\mathrm{B},1})$ to arrive at the simple expression

$$\frac{F}{nk_\mathrm{B}T} \approx \frac{F_0}{nk_\mathrm{B}T} + \frac{1}{2}R_{11}{\phi_{\mathrm{A},1}}^2 + R_{12}\phi_{\mathrm{A},1}\phi_{\mathrm{B},1} + \frac{1}{2}R_{22}{\phi_{\mathrm{B},1}}^2 \tag{40}$$

where F_0 is the free energy of the uniform disordered phase and

$$R_{11} = \frac{S_{22}}{\det(S)\phi} + \frac{1}{\alpha(1 - \phi)} - 2\chi_{\mathrm{AS}}N \tag{41}$$

$$R_{12} = \frac{-S_{12}}{\det(S)\phi} + \frac{1}{\alpha(1 - \phi)} + \chi_{\mathrm{AB}}N - \chi_{\mathrm{AS}}N - \chi_{\mathrm{BS}}N \tag{42}$$

$$R_{22} = \frac{S_{11}}{\det(S)\phi} + \frac{1}{\alpha(1 - \phi)} - 2\chi_{\mathrm{BS}}N \tag{43}$$

Given the functional form of eq 40, it immediately follows that the disordered state (i.e., $\phi_{\mathrm{A},1} = \phi_{\mathrm{B},1} = 0$) is metastable (i.e., is a local minimum) if and only if

$$R_{11}R_{22} > {R_{12}}^2 \tag{44}$$

for all $x \equiv k^2a^2N/6$. The spinodal, which coincides with the lamellar to disorder transition, occurs at the first point where an x exists such that $R_{11}R_{22} = R_{12}^2$. This special value of x is labeled x^*, and is related to the lamellar period in the vicinity of the ODT by $D = 2\pi a\sqrt{N/6x^*}$. Furthermore, the ratio $\phi_{\mathrm{A},1}/\phi_{\mathrm{B},1}$ near the ODT is given by $-R_{11}/R_{22}$, from which it follows that

$$\frac{\sigma_\mathrm{S}}{\sigma_{\mathrm{AB}}} = \frac{R_{11} - R_{22}}{R_{11} + R_{22}} \tag{45}$$

Indeed, these results all match up perfectly with our full SCFT calculations.

References and Notes

(1) Matsen, M. W.; Bates, F. S. *Macromolecules* **1996**, *29*, 1091.
(2) Fredrickson, G. H.; Helfand, E. *Macromolecules* **1987**, *87*, 697.
(3) Zhao, J.; Majumdar, B.; Schulz, M. F.; Bates, F. S.; Almdal, K.; Mortensen, K.; Hajduk, D. A.; Gruner, S. M. *Macromolecules* **1996**, *29*, 1204. Schulz, M. F.; Khandpur, A. K.; Matsen, M. W.; Bates, F. S.; Almdal, K.; Mortensen, K.; Hajduk, D. A. Unpublished material.
(4) Shi, A.-C.; Noolandi, J. *Macromolecules* **1995**, *28*, 3103. Matsen, M. W.; Bates, F. S. *Macromolecules* **1995**, *28*, 7298.
(5) Helfand, E.; Tagami, Y. *J. Chem. Phys.* **1972**, *56*, 3592.
(6) Huang, C.-I.; Lodge, T. P. *Macromolecules* **1998**, *31*, 3556.
(7) Huang, C.-I.; Chapman, B. R.; Lodge, T. P. *Macromolecules* **1998**, *31*, 9384.
(8) Hashimoto, T.; Shibayama, M.; Kawai, H. *Macromolecules* **1983**, *16*, 1093.

(9) Mori, K.; Atsuo, O.; Hashimoto, T. *J. Chem. Phys.* **1996**, *104*, 7765.
(10) Hanley, K. J.; Lodge, T. P.; Huang, C.-I. *Macromolecules* **2000**, *33*, 5918.
(11) Hanley, K. J.; Lodge, T. P. *J. Polym. Sci., Part B* **1998**, *36*, 3101. Sakurai, S.; Hashimoto, T.; Fetters, L. J. *Macromolecules* **1996**, *29*, 740.
(12) Lodge, T. P.; Pan, C.; Jin, X.; Liu, Z.; Zhao, J.; Maurer, W. W.; Bates, F. S. *J. Polym. Sci., Part B* **1995**, *33*, 2289.
(13) Shibayama, M.; Hashimoto, T.; Hasegawa, H.; Kawai, H. *Macromolecules* **1983**, *16*, 1427. Hashimoto, T.; Mori, K. *Macromolecules* **1990**, *23*, 5347. Sakamoto, N.; Hashimoto, T.; Han, C. D.; Kim, D.; Vaidya, N. Y. *Macromolecules* **1997**, *30*, 5321.
(14) Fredrickson, G. H.; Leibler, L. *Macromolecules* **1989**, *22*, 1238.
(15) Leibler, L. *Macromolecules* **1980**, *13*, 1602.
(16) De Gennes, P.-G. *Scaling Concepts in Polymer Physics*; Cornell University Press: Ithaca, NY, 1979.
(17) Whitmore, M. D.; Vavasour, J. D. *Macromolecules* **1992**, *25*, 2041.
(18) Whitmore, M. D.; Noolandi, J. *J. Chem. Phys.* **1990**, *93*, 2946.
(19) Helfand, E. *J. Chem. Phys.* **1975**, *62*, 999.
(20) Banaszak, M.; Whitmore, M. D. *Macromolecules* **1992**, *25*, 3406.
(21) Matsen, M. W.; Bates, F. S. *J. Polym. Sci., Part B* **1997**, *35*, 945.
(22) Matsen, M. W. *J. Phys.: Condens. Matter.* **2002**, *14*, R21.
(23) Doi, M. *Introduction to Polymer Physics*; Oxford University Press: Oxford, U.K., 1996.
(24) Matsen, M. W. *Phys. Rev. Lett.* **1995**, *74*, 4225.
(25) Lodge, T. P.; Hamersky, M. W.; Hanley, K. J.; Huang, C.-I. *Macromolecules* **1997**, *30*, 6139.
(26) Olvera de la Cruz, M. *J. Chem. Phys.* **1989**, *90*, 1995.
(27) Mayes, A. M.; Barker, J. G.; Russell, T. P. *J. Phys. Chem.* **1994**, *101*, 5213.
(28) Maurer, W. W.; Bates, F. S.; Lodge, T. P.; Almdal, K.; Mortensen, K.; Fredrickson, G. H. *J. Chem. Phys.* **1998**, *108*, 2989. Buzza, D. M. A.; Hamley, I. W.; Fzea, A. H.; Moniruzzaman, M.; Allgaier, J. B.; Young, R. N.; Olmsted, P. D.; McLeish, T. C. B. *Macromolecules* **1999**, *32*, 7483.

MA0122066